Spatially resolved soil solution chemistry in a central European atmospherically polluted high-elevation catchment

5 Daniel A. Petrash[1], Frantisek Buzek[1], Martin Novak[1], Bohuslava Cejkova[1], Pavel Kram[1], Tomas Chuman[1], Jan Curik[1], Frantisek Veselovsky[2], Marketa Stepanova[1], Oldrich Myska[1], Pavla Holeckova[1], Leona Bohdalkova[1]

[1] Czech Geological Survey, Department of Environmental Geochemistry and Biogeochemistry, Geologicka 6, 152 00, Prague 5, Czech Republic
10 [2] Czech Geological Survey, Department of Rock Geochemistry, Geologicka 6, 152 00, Prague 5, Czech Republic

Correspondence to: Daniel A. Petrash (daniel.petras@geology.cz)

Abstract. To interpret spatial patterns of soil nutrient partitioning and compare these with runoff in a temperate forest with a history of acidification-related spruce die-back, the chemistry of mineral soil solutions were collected by suction lysimeters and evaluated relative to concurrent loads of anions and cations in precipitation. Lysimeters nest were installed in the 33-ha U
15 dvou loucek (UDL) mountain catchment at different topographic positions (hilltops, slopes and valley). Following equilibration, monthly soil solution samples were collected over a 2-year period. In the vicinity of each lysimeter nest, soil pits were excavated for constraining soil chemistry. Soil solutions were analyzed for SO_4^{2-}, NO_3^-, NH_4^+, Na+, K^+, Ca^{2+}, Mg^{2+}, and total dissolved Al concentrations and organic matter (DOC), and pH. For a P release estimation, ammonium oxalate extraction of soil samples was performed. Comparison of soil water data with other previously acidified monitored European sites
20 indicated that environmentally relevant chemical species at UDL had concentrations similar to median concentrations observed in sites with similar bedrock lithology and vegetation cover. Cation exchange capacity (CEC $\leq$ 58 meq kg^{-1}) and base saturation (BS $\leq$ 13 %), however, were significantly lower at UDL, documenting incomplete recovery from acidification. Spatial trends and seasonality in soil water chemistry support belowground inputs from mineral-stabilized legacy pollutants. Overall, the soil-solution data suggest the system is out of balance chemically, relative to the present loads of anions and cations in
25 precipitation. Higher concentrations of SO_4^{2-}, NO_3^-, and base cations in runoff than in soil solutions are explained by lateral surficial leaching of pollutants and nutrients from shallow soil horizons. Nearly 30 years after peak acidification, UDL exhibited similar soil solution concentrations of SO_4^2, Ca^{2+} and Mg^{2+} as median values at the Pan-European International Co-operative Program (ICP) Forest sites, yet NO_3^- concentrations were an order of magnitude higher.

1 Introduction

30 In the mid-20th century, high anthropogenic emissions of sulfur dioxide (SO_2) and nitrogen oxides (NO_x) produced sulfuric and nitric acids (H_2SO_4, HNO_3) that affected forest ecosystems via wet and dry deposition. The largest point sources of these

compounds were coal-burning power plants (Blazkova et al., 1996; Kolar et al., 2015). In central Europe alone, acid rain killed spruce stands on an area of approximately 1000 km^2 in the so-called "Black Triangle", which includes mountainous border regions of three countries: Czech Republic, East Germany and Poland (Blazkova et al., 1996). Emissions of acidifying compounds in these centrally planned economies peaked in the late 1980s; installation of desulfurization units in coal-burning

5   power plants was completed in the mid-1990s in the Czech Republic and Germany, and several years later in southern Poland (Fen et al., 1998; Alewell et al., 2001; Hruska et al. 2003). As in other forest ecosystems negatively affected by acid rain, in the Black Triangle area the productivity of temperate forests was perturbed by (i) enhanced leaching of base cations, such as potassium (K^+), calcium (Ca^{2+}) and magnesium (Mg^{2+}) (e.g., Gradowski et al., 2008, Kopacek et al., 2015), and (ii) decreased bioavailability of phosphorous (P), an important macronutrient (Matschullat et al., 1998).

10   UDL is a heavily acidified, mountain-slope catchment in the northeastern Czech Republic (Fig. 1). It is situated on base-poor crystalline bedrock located within the Black Triangle area (Fig. 1a). Amongst 14 multi-decadal monitored small forested catchments of the Czech' GEOMON network, UDL received the highest bulk atmospheric loads of a variety of pollutants, in particular nitrogen and sulfur. As a result, the catchment is P limited and N saturated, with the pollution recovery process apparently altering concentrations and fluxes of other solutes (Oulehle et al., 2017).

15   To interpret temporal and spatial relations between environmentally relevant chemical species of soil nutrient partitioning and compare these with runoff in a temperate forest with a history of acidification-related spruce die-back, the chemistry of mineral soil solutions were collected by suction lysimeters and evaluated relative to concurrent loads of anions and cations in precipitation and runoff. For this aim, a nests of suction lysimeters was installed along both slopes of the V-shaped UDL valley and measurements started after one year equilibration period. The resulting dataset documents spatially variable nutrient

20   imbalances in podzolized soils following the retreat of peak acidification. When evaluated with regard to runoff, and previously published input and fluxes data (i.e., Oulehle et al., 2017), our data provide insights into the localized controls and effects of acidification disturbances, and offer a perspective of the spatially and temporarily variable nutrient concentrations at a catchment-scale. Comparative figures on strong anion inputs and leaching of base metals and acid anions reflect nutrient imbalances linked to groundwater carrying legacy pollutants. Insights from this study are relevant for evaluating soil recovery

25   processes after atmospherically induced perturbations of podzolized soils.

2 Materials and Methods

2.1 Study Site

This study was conducted in the UDL (U dvou loucek) catchment, NE Bohemia, Czech Republic. Located in the Eagle Mountains (Orlicke hory) at coordinates 50°13′ N, 16°29′ E (Fig. 1a), UDL is a 33-ha, V-shaped valley (Fig. 1b), incised

30   within alkaline orthogneiss (SiO_2 = 75 wt. %; $Na_2O + K_2O$ = 8 wt. %; $MgO + CaO$ < 0.5 wt. %). This lithology, together with blue schists of Neoproterozoic sedimentary protoliths, comprise the Orlica-Snieznik Massif. U-Pb and Pb/Pb isochrones of the orthogneiss point to a Cambro-Ordovician protolith (Winchester et al., 2002; Don et al., 2003). With an elevation of 880-950

m, UDL's climate is characterized as humid temperate. Low base status soils (Entic Podzols) have developed at expense of the parental porphyritic granite, and Mor is the most common humus form (Oulehle et al., 2017). The mean precipitation is 1500 mm yr^{-1}, and the mean annual air temperature is 5.0 °C. An ephemeral snow cover lasts from late November to late March, when the highest runoff flow is usually recorded (~162 ± 29 mm). Historically, the site was influenced by emissions

5 from large industrial complexes in the nearby Polish Silesia, where technological upgrades in abundant coal-burning power plants were introduced later than in the Czech Republic.

UDL is also one of only three monitored catchments in the Czech Republic whose forests were affected by massive acidification-related spruce die-back. It experienced several episodes of spruce die-back between 1975 and 1996, and its current vegetation cover includes approximately 27% of young Norway spruce (saplings < 40 yrs) following reforestation,

10 with 1.7 out of 33 ha being non-forested (Oulehle et al., 2017). Following spruce defoliation, liming by aircraft was performed three times to raise the soil pH. Liming took place in 1986, 2002 and 2007, introducing three metric tons of ground dolomitic limestone per hectare into the mountain ecosystem on each occasion. The. During the decade 1994-2014, the soil pH$_{H2O}$ in UDL remained stable in the range 4.92 ± 0.40. Over the same period, a pH increases in throughfall measurements compile by Oulehle et al. (2017) from 4.07 to 5.19 was registered across the Czech Republic (Oulehle et al., 2017). At times of peak soil

15 acidification, recorded, yet unpublished pH$_{KCl}$ measurements were below 3 units (Hruska, 2000).

Annual hydrochemical input-output mass balances for this site have been recently revised and compared with those of other monitored catchments in the Czech Republic (Oulehle et al., 2017). Historical input-output hydrochemical data are summarized in Table 1, and time-series of concentration data for base cations, nitrate (NO$_3^-$) and sulfate (SO$_4^{2-}$) are shown in Figure 2. The stream's pH was consistently acidic (< 5.5). For most elements (except for Na$^+$), the highest concentrations were observed in

20 spruce canopy throughfall, followed by runoff (SO$_4^{2-}$, Ca^{2+}, Mg^{2+}, K$^+$) and open-area precipitation (NO$_3^-$). The average (1994-2014) sulfur (S) bulk atmospheric input was ~1.6 g m^{-2} year^{-1}, which is far in excess of the atmospheric input in the remaining 13 monitored catchments (Oulehle et al., 2017) across the Czech Republic (0.75 g m^{-2} year^{-1}). Dissolved inorganic nitrogen (DIN) deposition input was 11.7 mg m^{-2} year^{-1}, exceeding the value observed at other monitored sites. The Ca^{2+} input of 2.5 g m^{-2} year^{-1} largely exceeded the average Ca^{2+} input into other monitored catchments (0.6 g m^{-2} year^{-1}). The Mg^{2+} catchment

25 input into UDL was 0.3 g m^{-2} year^{-1} (the average for all sites of the monitoring network was 0.1 g m^{-2} year^{-1}). Inputs of Na$^+$ and K$^+$ were 0.6 and 1.3 g m^{-2} year^{-1}, respectively (averages across 14 sites were 0.2 and 0.5 g m^{-2} year^{-1}).

2.2.1 Soil solution samples

In October 2010, five nests of Prenart suction lysimeters were installed at a 50-cm depth below soil surface in a V-shaped arrangement as follows: hilltop west, hilltop east, slope west, slope east, and valley (filled circles in Figure 1b). The lysimeter

30 distributions along the V-shaped Shale Hills Critical Zone Observatory (Pennsylvania, USA (see Ma et al., 2015; Brantley et al., 2018) inspired our sampling design at UDL. Each nest consisted of three lysimeters, 6 to 10 m apart. During the first 12 months, soil solutions were collected each month and discarded. Monthly hydrochemical monitoring of soil solutions was then

performed during the following two hydrological years, i.e., from November 2011 to October 2013. A total of 15 replicates (3 per sampling location) were collected monthly.

2.2.2 Soil Samples

Five 0.5 m^2 soil pits were excavated using the methodology described by Huntington et al. (1988) along both slopes of the
UDL catchment (open circles in Figure 1b). Forest floor and mineral soil were removed to a depth of > 80 cm below surface, and separated into the Oi/(L) + Oe(F) and Oa(H) layers, and four mineral soil horizons defined by depth (0-10, 10-20, 20-40, and 40-80 cm). Soil profiles were described following the guidelines of the Food and Agriculture Organization of the United Nations (FAO, 2006). The soil layers were weighed in the field, processed by sieving to stones; coarse roots; the > 1 cm soil fraction; and the < 1 cm soil fraction. Two kg of the < 1 cm soil fraction were transported to the laboratory. Only results from
the 40-80 cm mineral layer, which are considered to be in chemical equilibrium with our 50-cm depth lysimeters, were further processed as part of this research.

2.2.3 Bulk atmospheric deposition

Atmospheric deposition was sampled in an open area ("rainfall"). Cumulative monthly rainfall was collected in three replicates. The rainfall sampling sites are 20 m apart among them and 1.2 m above ground (open squares in Fig. 1b). Diffusive and
evaporative losses from narrow-mouth bulk rain collectors were avoided by keeping precipitation under a 5-mm layer of chemically stable mineral oil. Runoff samples were collected monthly at the limnigraph location (Fig. 1b).

2.3. Analyses

2.3.1. Soil Characterization

A Radiometer TTT-85 pH meter with a combination electrode was used to measure pH_{H2O} of soil. Soil moisture was determined
in the laboratory by difference of weights after 24 hrs of oven-drying at 105 ° C. Soil texture was analyzed by the hydrometer method (ISO 11277 2009). Following air drying, the substrate was sieved through a 2-mm sieve. The sieved samples were kept at 5 ° C before chemical analysis.

After centrifugation and filtration through 0.45 μm cellulose–acetate filters, the filtrates were analyzed for cations. Exchangeable H^+ and Al^{3+} were determined by NaOH neutralization titration following the $BaCl_2$ extraction. Exchangeable
ions (Na^+, K^+, Mg^{2+}, Ca^{2+},) were extracted from the < 2mm soil fraction with 0.1 mol L^{-1} $BaCl_2$ (solution : soil ratio of 50 : 1). Concentrations of NO_3^- and SO_4^{2-} were determined by ion chromatography (HPLC Knauer 1000; detection limits of 0.1 and 0.3 mg L^{-1}).

For a phosphorus (P) release estimation, ammonium oxalate extraction was performed (Schoumans, 2000). A reagent solution consisting of $(COONH_4)2 \cdot H_2O$ and $(COOH)_2 \cdot 2H_2O$ was used to dissolve 1 g of the < 2 mm soil fraction. After shaking for 2
h in the dark, centrifugation and filtration, the soil solutions were analyzed for total dissolved oxalate extractable phosphorus

(P_{ox}), iron (Fe_{ox}), and aluminum (Al_{ox}). These were used to estimate the degree of P saturation of the soil [$DPS = P_{ox}*(0.5*(Fe_{ox} + Al_{ox})^{-1})$], which accounts for the P available to be released into solution in relation to the remaining binding capacity of soil and, thus, allows identifying areas in the catchment with relatively higher potential for P export (Beauchemin et al., 1999; Borovec et al., 2018). For calculations of the amount of P sorbed by soil particles (Borovec et al., 2018), the average runoff P

5   concentration, measured during our two years monitoring period (i.e., 27.9 ± 6.5 µg L^{-1}), was used as an input for calculating the equilibrium P concentration in the catchment area.

2.3.2. Soil Solutions

Concentrations of NH_4^+ and total phosphorus (P_{tot}) were measured spectrophotometrically (Perkin-Elmer Lambda 25; > 20 and 6 µg L^{-1}, respectively). Concentrations of Na^+, K^+, Ca^{2+} and Mg^{2+} were determined by electrothermal atomic absorption

10   (AAnalyst 200; > 5 µg L^{-1}). Concentrations of aluminum (Al^{3+}) were also measured by electrothermal atomic absorption instrument with a graphite furnace (D.L. < 0.01 mg L^{-1}). Concentrations of DOC and total dissolved nitrogen (TN) were determined on a combustion analyzer (Torch, Teledyne Temar; D.L. < 0.1 and 0.5 mg L^{-1}).

2.4. Statistical Analysis

Non-parametric data were evaluated by factor analysis. Empirical data were implemented in the computer code XLSTAT

15   following the protocol by Vega et al. (1998). In short, data were normalized to zero and unit variance, and a covariance matrix of the normalized species was generated. For this analysis, the covariance matrix was diagonalized and the characteristic roots (eigenvalues) were obtained. The transformed variables, or principal components (PCs), were obtained as weighted linear combinations of the original plotted multidimensional variables. A rotation of principal components allowed simpler and more meaningful representation of the underlying factors by decreasing the contribution of each variables to the two-dimensional

20   plane. Variables then plotted in groups with correlation among them determined by their position (proximity). The two-dimensional plane where the rotated normalized data plotted can be interpreted in terms of the main controls over the general variance (see Vega et al., 1998 for details).

3. Results

3.1. Soil Texture and pH

25   Table 2 lists physical data for mineral soil and chemical data for soil extracts from the 40-80 cm depth layer and compares them with data for soil solutions collected by suction lysimeters (50-cm depth). Following the conceptual sampling purposed in Shale Hills Critical Zone Observatory, our dataset is grouped according to sampling' geographic location and position in the catchment area (i.e., hilltops, slopes and valley; Fig. 1). In the eastern part of the catchment, a coarse soil granulometry

comprised of pebbles and cobbles accounted for 24 % of soil particle size in the hillslope and 62 % at the hilltop, whereas in the western part of the catchment, the soil was sandy, with pebbles and cobbles accounting only for 12 %.

The 40-80 cm soil depth was characterized by acidic pH_{H2O} (Table 2). Mineral soil pH was higher in the valley (4.7), compared to the hilltop (4.2 to 4.4). The mean pH of soil solutions ranged similarly between the first and the second year, except for the valley (pH valley of 4.1 in year 1, and 4.5 in year 2; Table 2). The two-year averages of soil solutions were 5.2, 4.7, and 4.3 pH units on the hilltops, slopes, and valley, respectively. Therefore, the solid substrate extracts and soil solutions were characterized by an opposite elevational pH trend; i.e., more acidic substrate extracts uphill, more acidic soil water downhill.

3.2. Basic Soil Chemical Characterization

In the eastern part of the catchment, the cation exchange capacity (CEC) of the mineral soil at 40-80 cm depth was 33 meq kg^{-1} on the slope and 58 meq kg^{-1} on the hilltops (mean 32 meq kg^{-1}; Table 2). By contrast, in the western part CEC was 22 and 19 meq kg^{-1} on the slope and hilltops, respectively. CEC in the valley was 27 meq kg^{-1}. The range of base saturation (BS) values in the soil varied between 6 and 13 %, with higher BS observed in the east (> 9 %) as compared to the west (< 8 %). The CEC in the studied soil depth at UDL was dominated by exchangeable Al. Consequently, the soil base saturation (BS) and soil pH_{H2O} values were also low (Table 2).

BS at UDL was classified as poor with the dominant equivalent proportion of divalent base cations Ca (mean 46 %) and Mg (mean 24 %). The BS at UDL was twice larger than the BS in similar soil depths in the leucogranitic catchment LYS (Kram et al., 1997; Hruska et al., 2001), which is the most acidified catchment of the Czech monitoring network (Oulehle et al., 2017). Holmberg et al. (2018) evaluated BS and CEC of numerous forest sites of the LTER (Long-Term Ecological Research) network in nine European countries, with calculated median BS of 30 % and CEC of 84 meq kg^{-1}. From the European perspective, the soil BS and CEC values at the UDL were low.

Oxalate-extractable P was the lowest in the valley (334 mg kg^{-1}), and highest on hilltop east (536 mg kg^{-1}). The degree of P saturation varied between 0.08 (valley) and 0.16 (hilltop east). These values fall below the lowest range observed in soil plots of the Czech Republic (see Borovec et al., 2018). Concentrations of organic C (C_{org}) ranged between 0.40 and 1.81 wt. %, while concentrations of total nitrogen (TN) were between 0.02 and 0.10 wt. %. Concentrations of both C_{org} and TN were the highest on hilltop east, and the lowest on hilltop west (Table 2).

3.3 Solute Concentrations in Soil Waters

Table 2 lists mean concentrations of major anions and cations in soil solutions, grouped according to sampling location and position in the catchment area (cf., Fig. 1). Mean concentrations of individual chemical species in soil solutions are listed separately for the years 2012 and 2013; whilst Figure S1 shows the spatial variability of the statistical distribution (minimum, first quartile, median, third quartile and maximum) for soil solutions concentrations of dissolved organic carbon, sulfate, nitrate, base cations, aluminum, chloride (in mg L^{-1}) and pH values at the 50-cm depth at UDL. Coefficients of variation within individual nests of lysimeters are listed in Table S1.

Our combined dataset (*i.e.,* Tables 1 and 2) show that six of the studied chemical species were more diluted in 50-cm soil waters than in runoff. Sulfate concentrations in soil waters were, on average, 37 % lower than those in runoff, while, relative to runoff, NO_3^- concentrations in soil waters were 14 % lower than those measured in runoff. Similarly, the concentrations of K^+, Na^+, Ca^{2+} and Mg^{2+} were lower in soil waters by 73, 63, 79 and 4 %, respectively. Water volumes collected by suction

5   lysimeters differed among sampling locations, decreasing from the hilltops to the slopes to the valley (means of 1.13, 0.99 and 0.38 L per lysimeter per month, respectively).

3.3.1. Anion Concentrations

A time-series plot reveals that SO_4^{2-} concentrations in the valley were higher in winter than in summer (Figure 3). The mean SO_4^{2-} concentrations in soil water during the monitored period were found to be higher at the slopes (East > West), followed

10   by the valley and hilltops (East ≈ West) (Table 2, Fig. S1). Our results for NO_3^- across the lysimeter network also show that this chemical species was readily bioavailable along mostly in the valley, where its concentrations were one order of magnitude higher than in the upslope soil solutions (Fig. S1). For this anion, the dataset also shows a high temporal variability, and in both years, NO_3^- concentrations in the valley peaked by late spring (Fig. 3). By comparison, the belowground NH_4^+ concentrations were found to be low (usually below the detection limit, Table 2), a result that is consistent with previous

15   observations at a soil research plot in north-western Czech Republic (Oulehle et al., 2006). For SO_4^{2-} and NO_3^-, coefficients of variation were between 2 and 17 %, with no clear-cut differences within the sampling locations (Table S1).

3.3.2 Cation Concentrations

Mean Na^+ and K^+ concentrations in soil solutions were the highest on slope east, close to 1.0 and 0.4 mg L^{-1}, respectively (Table 2; Fig. S1). For these cations, coefficients of variation (Table S1) were between 9 and 55 %, with the hilltop soil waters

20   exhibiting the largest variation in K^+ concentrations. The second year was characterized by generally lower K^+ concentrations in soil solutions collected in the valley, compared to the first year. Na^+ concentrations in soil solutions in the valley started to decrease only in the second half of the second year (Fig. 3). The highest mean Mg^{2+} concentrations were observed on hilltop west (0.95 mg L^{-1}), the highest mean Ca^{2+} concentrations were measured on slope east (0.83 mg L^{-1}). The lowest mean Mg^{2+} concentrations were found in the valley (0.41 mg L^{-1}). The lowest mean Ca^{2+} concentrations were found also in the valley

25   (0.48 mg L^{-1}; Table 2, Figure S1). Coefficients of variations for Mg^{2+} and Ca^{2+} in soil solutions were relatively low, between 6 and 21 % (Table S1). The time series of Ca^{2+} concentrations exhibited localized maxima in spring/early summer of the second year in soil solutions collected in most locations. Except for slope east, most locations also exhibited indistinct maxima in Mg^{2+} concentrations in soil solutions in the spring/early summer of the second monitored year (Fig. 3).

3.4 Statistical Analysis

30   Several spatial trends are evident by evaluating the statistical distribution of anions and cations in the soil solutions (Table 2; Fig. S1). There was a weak correlation between atmospheric deposition, runoff and soil solution concentrations throughout the

monitored period (Fig. S2). The first factor of our explorative factor analysis, D1, exhibited a maximal overall variance that explained 19 % of total inter-correlated variance of collected data. The second factor, D2, had maximal variance amongst all unit length linear combinations that were uncorrelated to D1 and explained 12 % of variance within the dataset (Fig. S1). Based on the weights of the parameters, correspondence to each of these factors, and their cluster distribution, intrinsic properties of

5 the soil, such as its DOC and clay contents (i.e., D1), determined the variance on the soil water solute concentration to a higher degree (i.e., 19 %) than seasonal inputs (i.e., D2). In summary, given the complexity of the possible interrelations among the environmental variables considered, there was an apparent insignificant correlation between solute the concentrations measured in the soil in 2012-2013, runoff and atmospheric deposition data. Such a result in turn points to a major control exerted by groundwater chemistry over soil water chemistry, and also to soil organic and inorganic ligand properties that also

10 exert a control over the residence time of each of the measured component. The contribution of groundwater *vs.* runoff infiltration is further by evaluated mean of an isotopic runoff model in the Appendix A.

4. Discussion

4.1 Comparison with Other European Forests

A comparison of previous studies with data presented here is not straightforward due to differences in sampling and analytical

15 strategies, dissimilar and heterogeneous bedrock lithologies, variable soil buffering capacities, and other factors, such as canopy density, inter-annual water influx variability, and tree species diversity. Nonetheless, insights from the studies provide the framework for our interpretations. Johnson et al. (2018) have recently published soil solution data from 162 plots monitored as part of the (ICP) Forest monitoring network, including median concentrations of environmentally relevant chemical species for the years 1998-2012. Soil solutions in the 40-80 cm deep mineral subsoil across Europe typically contained 6.3 mg SO_4^{2-}

20 L^{-1}, 1.0 mg NO_3^- L^{-1}, 1.9 mg Ca^{2+} L^{-1}, and 0.7 mg Mg^{2+} L^{-1}. It follows that soil solutions at UDL in 2012-2013 were characterized by similar concentrations of SO_4^{2-}, Ca^{2+} and Mg^{2+} as the ICP sites, and by an order of magnitude higher NO_3^- concentrations than the ICP sites. Solute concentrations in UDL are also above those observed in other studies that evaluated temporal changes in inputs, runoff and soil solution chemistry and fluxes in analogous forest ecosystems (e.g., Manderscheid et al., 1995a,b; Wesselink et al., 1995, Hruska et al., 2000; Armbruster et al., 2004; Oulehle et al., 2006; Navratil et al., 2007).

25 ### 4.2 Spatial and Temporal Variability in UDL Soil Water Chemistry

In all studied soil solutions, an elevational trend was found in soil water parameters, such as pH, DOC and the concentrations of Ca^{2+}, and Mg^{2+}. All these parameters showed a decreasing trend downhill, with evident spatial trends in the soil solution chemistries (Table 2; Figures 3 and S1). Amongst these trends were those for pH (a 0.6 units difference), and DOC (concentrations on the hilltop of approximately 14 mg L^{-1}, lower by a factor of 2 to 3 in the valley). In contrast, the decrease

30 in Ca^{2+} and Mg^{2+} concentrations in soil solutions downslope was small, within 1 mg L^{-1}. Clear-cut seasonal concentration

trends in soil solutions were recorded for NO_3^- and SO_4^{2-} (valley and slope west; Table 2). The underlying mechanism may be different for both anions.

A co-evaluation of peak nitrate levels in soil solutions and precipitation during the monitoring period (Fig. S3) do not suggest a cause effect-relation linked to dry deposition. Thus, higher abundance of NO_3^- in soil solutions in the growing season may

5 be related to higher rates of nitrification of organically cycled NH_4^+-N during summer (van Miegroet and Cole, 1984). Higher abundance of SO_4^{2-} in soil solutions in winter remains unexplained. Historically, more S pollution was caused by higher SO_x emission from coal-burning power plants during the heating season, but such seasonality was no longer seen for the years 2012-2013 (Fig. 2). High nitrate in soil solutions during summer originated during the dormant season, and high sulfate concentrations observed during the winter, originating from recycled organic S during the summer (Meyer et al, 2001; Novak

10 et al., 2001).

Toward the hilltops, differences in porosity and greater fluid–rock-derived particle interactions, together with higher reactive surface area and solute flux may exert a control over the measured soil solution chemical variability (Godsey et al., 2009). The latter effect seems to be critical in the variability in soil solution chemistry as the hilltop' lower soil horizons, which are sandy and contain significant amounts of coarse parental-rock material (Table 2). For DOC, the high variability on the slopes may

15 reflect preferential flow paths. The higher DOC belowground leaching on the eastern hilltop suggest that C partitioning is site-specific, with little lateral redistribution from upslope organic soil horizons toward the valley.

Due to successful pollution abatement strategies, atmospheric input has decreased since peak acidification, and UDL has been characterized by higher export of SO_4^{2-}, DOC, Ca^{2+}, Mg^{2+}, K^+, and Na^+ than their atmospheric input. Conversely, export of total inorganic N from UDL *via* stream runoff continues to be significantly lower than its atmospheric input (Oulehle et al.,

20 2017). As shown by Novak et al. (2004) using sulfur isotope ratios ($^{34}S/^{32}S$), cycling of the high amounts of deposited SO_x at UDL occurred not only by adsorption/desorption of SO_4^{2-} on soil particles, but, to a great extent, also by cycling through the soil organic matter, which may prevail for several decades (Novak et al., 2000; Armbruster et al., 2003; Mörth et al., 2005). In UDL, decreased NO_3^- export is controlled by biological processes, rather than catchment hydrology (Oulehle et al., 2017). Invasion of hardwood species to UDL following spruce dieback, along with an increase in total (aboveground) biomass,

25 continue to immobilize a large proportion of the deposited NO_3^- and NH_4^+ (see McDowell et al., 2004). This is nicely illustrated by limited presence of dissolved inorganic N forms in our soil solution chemistries (Table 2; Figure 3).

Within our time series, Ca^{2+} and Mg^{2+} concentrations in soil waters defined a general trend that likely reflect the balance between evapotranspiration and biological inputs, with a punctual, correlative shift recorded in concentrations measured during mid-2013 (Table 2). These seemed coeval to increased inputs in strong anions (Fig. 2). Increased leaching of these

30 macronutrients could also be regulated by temporary changes in soil nitrate abundances (Oulehle et al., 2006; Wesselink et al., 1995; Akselsson et al., 2007, 2008). Whilst factor analysis did not reveal significant relationships between measured UDL parameters (Fig. S1), cross-plots in Figure 4 show a relatively strong pH–Mg/Al correlation. Both variables in each cross-plot reached the highest values on slope east and the lowest values in the valley. Thus, correlations seem to follow a trend determined by the higher Al solubility at lower pH (Palmer et al., 2005).

4.3 Retreat of Acidification

Our spatially resolved time-series observations for soil solution Na^+ and K^+ (Fig. 3) show that the concentrations of these ions defined patterns and trends largely derived from heterogeneity in soil textures (Table 2), with seasonality and pulses in atmospheric inputs also exerting a likely areal control over average and peak concentrations (Fig. 2). For K^+, and to a minor

5   extent for Na^+, soil water concentrations recorded peaks that are more or less correlative to SO_4^{2-} and NO_3^- inputs (cf., Figs. 2 and 3), again pointing to lapses in which the atmospheric contributions of strong anions exerted a significant control over the weathering and leaching of plagioclase and K-feldspars in the underlying crystalline rock; for example (Moore et al., 2012). In this regard, Oulehle et al. (2017) reported that K^+ average annual runoff through runoff was two to three times higher than that of Na^+ (Table 1), with both cations exceeding runoff concentrations values measured in other monitored catchments.

10 When localized variations in Na^+ and K^+ at the 50 cm-depth soil solutions at UDL are evaluated, a deep flow path within the eastern slope to the valley seems possibly augmented as a response of either atmospheric S inputs or solubilization of the SO_4^{2-} stored in the weathering zone below the rooted soils, due to water saturation of the soil. Because Na^+ has low affinity toward organic and inorganic ligands in soil, and thus behaves relatively conservatively (McIntosh et al., 2017), a seemingly more rapid response of Na^+ leaching to soil solution could result from strong anion accumulation toward the relatively more humid

15 spring season of 2013 (Fig. 3). Such observation can in turn be interpreted as a decrease in water residence time from the slope to the valley. This effect is probably linked to increased soil water saturation and concomitant increase in the hydrologic connectivity of soil pore waters to the stream, with a heterogeneous distribution of dissolved ions in soil solutions at the catchment-scale (Basu et al., 2010).

4.4 Phosphorus Availability and Belowground Organic Matter Allocation

20 Soil P sorption saturation is often used as an environmental indicator of soil P availability to runoff. Phosphorus losses from soils not subjected to an augmented erosional process are generally small (see Heuck et al., 2016 for a discussion). Our calculation of P sorbed by the soil particles, as determined by oxalate extraction (after Borovec et al., 2018), shows that between 22 and 29 mg of P per kg of soil was sorbed in the 50 cm-depth at the time of sampling, with insignificant difference between hilltops, slopes and valley. That contrasts with elevational differences in DOC concentrations in soil solutions seen in Fig. 3;

25 P and C_{org} in UDL soils at the studied depth are de-coupled.

5. Conclusions

Cation exchange capacity in UDL soils developed on base-poor orthogneiss ranged between 19 and 58 meq kg^{-1}, base saturation was 6-13 %. Both parameters had lower values than median values at the European LTER sites (84 meq kg^{-1} and 30

30 %, respectively).

Soil solutions at the 50-cm depth were generally more diluted than stream runoff. This can be explained by lateral surface runoff of solutions originating in the litter and humus, enriched in SO_4^{2-}, NO_3^-, K^+, Na^+, Ca^{2+} and Mg^{2+} due to anthropogenic atmosphere-derived pollution and/or as a result of natural biogeochemical processes that can be enhanced by increased periods of drought and more frequent torrential rains. Soil solutions had lower pH in the valley than at upslope locations, and were

5   more diluted in the valley than on hilltops in the case of DOC, Ca^{2+} and Mg^{2+}. In the valley, NO_3^- and SO_4^{2-} in soil solutions exhibited a clear seasonality, with maximum concentrations in the growing and dormant season, respectively. Phosphorus availability appeared to be decoupled from DOC. Differences between chemistry of soil water and runoff could have been caused by: (i) a direct contribution of throughfall, which scavenged atmospheric chemicals due to a large surface area of the canopy and leached nutrients from inside the foliage, or (ii) by polluted open-area precipitation, such surface runoff has been

10   documented especially along slopes considerably steeper than those at UDL.

Biogeochemical process within the soil which release more non-conservative ions than received from the atmosphere.

A contribution of groundwater enriched in selected chemical species due to sufficiently long water-rock interaction.

Finally, isotope investigations would be needed for better identification of dispersion pathways of Ca^{2+} and Mg^{2+} in the stressed ecosystem.

15   **Supplementary Materials:** The following are available online at ___, Figure S1 Descriptive statistics (2012- 2013) for soil water concentration values of dissolved organic carbon, sulfate, nitrate, base cations, Al and chloride (in mg L^{-1}) and pH values at the 50-cm depth at UDL. Figure S2: Non-parametric multidimensional scaling ordination of time-series hydrochemical data for runoff, atmospheric in lysimeters. Figure S3: Comparison of monthly precipitation volumes at UDL during the monitoring period (2012-2013) *vs*. the hydrologic years 2016-2017. Table S1: Coefficient of variation (Cv = $100\sigma/\mu$) of inorganic species

20   across our lysimeter network.

Author Contributions: Conceptualization, writing—review and editing D.P, M.N.; methodology F.B., M.N., data acquisition/validation, J.C., F.V., B.C., J.C., O.M., F,V., L.B.; visualization, M.S; formal analysis and investigation, D.P., P.H.; writing—original draft preparation, D.P., P.H., P.K.; writing—review and editing, DP, M.N and P.K.

Funding: This research was funded by Czech Science Foundation (GACR), grant number 18-15498S.

25   **Acknowledgments:** We express our gratitude for the constructive criticism of two anonymous reviewers which greatly improved the quality of this manuscript. Jakub Hruska and Tomas Navratil provided liming maps of the Eagle Mts. and data on oxalate extractions, respectively. We are grateful to Filip Oulehle for providing input/output hydrochemical data and his constructive criticism that helped improving an earlier version of this manuscript.

Conflicts of Interest: The authors declare no conflict of interest.

Appendix A

A1 Hydraulic insights from $^{18}O/^{16}O$ isotope modeling

Aiming at constraining the hydraulic parameters of the catchment under evaluation, a runoff generation model based on the water years 2016-2017, i.e., on a later time period, was constructed as we believe it compares to the soil solutions during 2012-

5   2013. To constrain the limitation of this approach, monthly precipitation among these periods ware compared. As seen in Figure S3, annual precipitation are comparable, with totals 1236, 1388, 1110, and 1284 mm in the hydrological years 2012, 2013, 2016 and 2017, respectively. Precipitation in the driest year 2016 corresponded to 80 % of precipitation in the wettest year 2013. Across this period, the mean monthly precipitation consistently peaked in December, May and September. Methodological details and mathematical components used to construct the isotopic $^{18}O/^{16}O$ model are provided in the

10   Appendix B (below).

Figure A1a shows that the $\delta^{18}O$ values of atmospheric input did not follow a canonical sinusoidal curve—isotopically heavy rainfall O in summer and isotopically light rainfall O in winter. Isotopically lighter H_2O-O in soil solutions relative to runoff in the spring of both years (Fig. A1b) indicate that water derived from the snowmelt predominates in soil pores several months toward summer. Isotopically heavier H_2O-O in soil water, common in summer of the first year and in autumn of the second

15   year, more closely corresponded to high $\delta^{18}O$ values of the instantaneous precipitation. Interestingly, $\delta^{18}O$ values of soil solutions in the valley (solid circles in Fig. A1) often departed from $\delta^{18}O$ values of runoff (thick solid line in Fig. A1b), despite the very small distance between the two sampling sites (70 m). Despite interpretative limitations imposed by different monitored periods, the runoff generation model can be generalized for the catchment interrogated here. Accordingly:

The response of the within-catchment hydrological system to precipitation is fast.

20   Runoff water at UDL is a mixture of direct precipitation with older soil water and even older shallow groundwater. The combination of all these three water types is called "mobile water", defined as the sum of all water pools and fluxes that respond to changing precipitation amounts.

The mean residence time of soil solutions calculated across all sampling locations indicate that the volume of the entire mobile water at UDL is larger than the volume of soil water transported under low vacuum to lysimeters 50 cm below surface.

25   The hydrochemistry at the 50-cm soil depth reflected a number of preceding precipitation events, modified by evapotranspiration and, to a much smaller extent, mineral dissolution; the mixture mostly remained in soil pore spaces until saturation was reached and leaching initiated; *cf.* Siegenthaler (1999).

The contribution of direct precipitation to runoff is relatively low: 5 to 35 % (Fig. A1c).

The mean residence time of water in the UDL catchment (~8.3 months) was shorter than in three previously studied catchments

30   in the Czech Republic. Lysina (LYS) catchment in the western Czech Republic (elevation of 830-950 m) was characterized by a mean water residence time of 15.2 months (Buzek 2009). Dehtare and Jenin catchments in the central Czech Republic (elevations of 500-640 and 640-880 m) had a mean water residence time of 12.5 and 9.3 months, respectively (Buzek et al., 1995). A fourth small catchment located in a spruce die-back affected area near Jezeri (northwestern Czech Republic; elevation

of 540-750 m) exhibited just slightly lower mean water residence time of 7.2 months than UDL (Maloszewski and Zuber 1982). While the bedrock at Jezeri and UDL was similar (gneiss), the steepness of both catchments differed (elevational span of 210 m at Jezeri *vs.* mere 70 m at UDL). The mean residence time of water at Jezeri and UDL was similar despite contrasting catchment areas (2.6 vs. 0.3 km^2).

5   **Appendix B**

B1 O isotope analyses

Atmospheric deposition was sampled in an open area ("rainfall"). Cumulative monthly rainfall was collected in three replicates, 20 m apart, 1.2 m above ground. Diffusive and evaporative losses from narrow-mouth rain collectors were avoided by keeping precipitation under a 5-mm layer of chemically stable mineral oil. Grab samples of runoff were collected monthly at the closing

10   profile. The $\delta^{18}O_{H2O}$ values were obtained by off-axis integrated cavity output spectroscopy (OA-ICOS; Liquid Water Isotope Analyzer, Model 3000, LGR Inc., Mountain View, Ca, U.S.A.). One µL of water was injected through a port heated to 80°C. The vapor was transported into a pre-evacuated cavity and analyzed for the $^{18}O/^{16}O$ ratio. The reproducibility of $\delta^{18}O_{H2O}$ determinations was better than 0.20 ‰.

B2. $\delta^{18}O_{H2O}$ modeling approach

15   A two-component model of runoff generation was produced using oxygen isotope ratios of H$_2$O ($\delta^{18}O_{H2O}$) of open-area precipitation, runoff and suction lysimeters water. The model is derived from a general isotope mass balance calculated following Eq. (1):

$$\delta^{18}O_{tot} = \frac{\sum \delta^{18}O_i * Q_i}{Q_{tot}} \quad [‰], \tag{1}$$

where i is an individual water source, Q$_i$ is its mass flow [m^3] and Q$_{tot}$ is the total flow [m^3]. This mass balance is typically

20   used for the separation of stormflow hydrograph into its event and pre-event components (Eq. (2)):

$$\delta_t Q_t = \delta_p Q_p + \delta_e Q_e \quad [‰. \text{m}^3.\text{s}^{-1}], \tag{2}$$

where Q$_t$ is streamflow [m^3.s^{-1}], Q$_p$ and Q$_e$ are contributing pre-event water (groundwater) and event water (rainfall, snowmelt) [m^3.s^{-1}], and δ_t, δ_p and δ_e are the corresponding isotopic compositions [‰]. Equation 2 can be solved parametrically for the contribution of the event water *p* and of the pre-event water (*1-p*) as shown in Eq. (3):

25    $$p = \frac{Q_e}{Q_t} = \frac{\delta_t - \delta_p}{\delta_e - \delta_p}. \tag{3}$$

The mass balance (1) is valid for any period of time if the isotope composition of all the components is known, for example for winter and summer. The mean annual $\delta^{18}O$ isotope composition (mean groundwater input), δ_{in}, was estimated as the mean $\delta^{18}O_{tot}$ of the runoff.

A simple method of estimating the turnover time (mean age) of the subsurface reservoir employs an exponential model approximation; the distribution of transit times of water in the outflow is exponential and likely corresponds to permeability decreasing with the aquifer depth (Maloszewski and Zuber, 1982; Buzek, 1991). In case of stable isotopes, Siegenthaler (1979) demonstrated that the input (*i.e.,* precipitation) can be approximated by a sinusoidal function with a one-year period as per Eq (4):

$$\delta_{precip} = D + A \sin (2\ \delta t), \tag{4}$$

where D = constant, A = amplitude of $\delta^{18}O$ variation in precipitation, t takes values 0-1 for a full-year period. Under a simplifying assumption of constant filtration and discharge, this input appears in discharge from the system as approximated by the factor B/A (Eq(5)):

$$\delta_{discharge} = D + B \sin (2\ \delta t + \delta), \tag{5}$$

where B is the amplitude of $\delta^{18}O$ variation in output (discharge) a δ is the time shift of output variations in relation to input. The mean transit time (T) in years can be determined using Eq. (6) either the damping factor B/A or the phase shift δ:

$$T = 1/2\ \delta\ ((B/A)^{-2} -1)^{1/2}. \tag{6}$$

A similar approach can be applied also to lysimeters; δ_{precip} represents the input, and infiltrated soil water (δ_{inf}) is used instead of $\delta_{discharge}$.

References

Akselsson, C.; Westling, O.; Alveteg, M.; Thelin, G.; Fransson, A.M.; Hellsten, S.: The influence of N load and harvest intensity on the risk of P limitation in Swedish forest soils, Sci. Total Environm. 404, 284–289. 2008.

Akselsson, C.; Westling, O.; Sverdrup, H.; Gundersen, P. Nutrient and carbon budgets in forest soils as decision support in sustainable forest management, Forest Ecol. Manag. 238, 167–174, 2007.

Alewell, C.: Predicting Reversibility of Acidification: The European Sulfur Story, Water Air Soil Pollut., 130, 1271–1276, 2001.

Armbruster, M.; Abiy, M.; Feger, K. H.: The biogeochemistry of two forested catchments in the Black Forest and the eastern Ore Mountains (Germany), Biogeochemisty 65, 341-368, 2003.

Armbruster, M.; Feger, K-H. Temporal trends in the chemical composition of precipitation, soil seepage and stream water in two forested catchments in the Black Forest and the eastern Ore, Monit, Nat. Environ. 5, 129-148, 2004.

Basu, N.B; Destouni, G.; Jawitz, J.W.; Thompson, S.E.; Loukinova, N.V., et al.: Nutrient loads exported from managed catchments reveal emergent biogeochemical stationarity, Geoph. Res. Lett. 37, doi.org/10.1029/2010GL045168, 2010.

Beauchemin, S.; Simard, R.R.: Soil phosphorus saturation degree, review of some indices and their suitability for P management in Québec, Canada, Can. J. Soil Sci. 79, 615–625. 1999,

5 Blazkova, M.: Black Triangle—The Most Polluted Part of Central Europe. In Regional Approaches to Water Pollution in the Environment; Rijtema P.E., Elias V. Eds.; NATO ASI Series 2, Environment, Kluwer Academic Publishers, Dordrecht, Volume 20, pp. 227-249, doi:10.1007/978-94-009-0345-6_11. 1996.

Borovec, J.; Jan, J.: Approach for predicting P sorption/desorption behaviour of potentially eroded topsoil in watercourses, Sci. Total Environ. 624, 1316–1324, 2018.

10 Brantley, S.L..; White, T.; West, N.; Williams, J.Z.; Forsythe, B.; Shapich, D.; Kaye, J.; Lin, H.; Shi, Y.; Kaye, M.; Herndon, E.: Susquehanna Shale Hills Critical Zone Observatory, Shale Hills in the context of Shaver's Creek watershed, Vadose Zone J. 17, 180092 , doi:10.2136/vzj2018.04.0092, 2018.

Buzek, F.; Hruska, J.; Kram, P.: Three component model of runoff generation, Lysina catchment, Czech Republic, Water Air Soil Pollut. 79, 391–408 1995.

15 Buzek, F.; Bystricky, V.; Kadlecova, R.; et al.: Application of two-component model of drainage discharge to nitrate contamination, J. Contam. Hydrol. 106, 99–117, 2009.

Buzek, F., Hanzlik, J.; Hruby, M.; Tryzna, P.: Evaluation of the runoff components on the slope of an open-cast mine by means of environmental isotopes ^{18}O and T, J. Hydrol. 127, 23–36, 1991.

Don, J.; Skacel, J.; Gotowala, R.: The boundary zone of the East and West Sudetes on the 1:50 000 scale geological map of 20 the Velke Vrbno, Stare Mesto and Snieżnik Metamorphic Units, Geologia Sudetica 35, 25-59, 2003.

Fenn, E.M.; Poth, M.A.; Aber, J.D.; Baron, J.S.; Bormann, B.T.; Johnson, D.W.; Lemly AD, McNulty SG, Ryan DF, Stottlemeye, R.: Nitrogen excess in North American ecosystems, predisposing factors, ecosystem responses and management strategies, Ecol. Applic. 8, 706–73, 1998.

Food and Agriculture Organization of the United Nations (FAO): The New Generation of Watershed Management 25 Programmes and Project; FAO Forestry Paper 150, Rome, Italy, 2006; pp. 128

Godsey, S.E.; Kirchner, J.W.; Clow, D.W.: Concentration–discharge relationships reflect chemostatic characteristics of US catchments, Hydrol. Proc. 23, 1844-1864. 2009.

Gradowski, T.; Thomas, S.C.: Responses of *Acer saccharum* canopy trees and samplings to P, K and lime additions under high N deposition, Tree Physiol. 28, 173–185, 2008.

30 Heuck, C.; Spohn, M.: Carbon, nitrogen and phosphorus net mineralization in organic horizons of temperate forests, stoichiometry and relations to organic matter quality, Biogeochemistry 131, 229–242, 2016.

Holmberg, M.; Aherne, J.; Austnes, K.; Beloica, J.; de Marco, A.; Dirnböck, T.; Fornasier, F.; Goergen, K.; Futter, M.; Lindroos, A.-J.; Kram, P.; Neirynck, J.; Pecka, T.; Posch, M.; Rowe, E.; Scheuschner, T.; Schlutow, A.; Valinia, S.; Forsius,

M.: Forest soil C, N and pH response to N and S deposition and climate change—a modelling study at European LTER sites, Sci. Total Environ. 640-641, 387–399, 2018.

Hruska, J.; Cudlin, P.; Kram, P.: Relationship between Norway spruce status and soil water base cations/aluminum ratios in the Czech Republic. In Acid Rain; Satake, K. et al. Eds.; Springer, Dordrecht; pp. 983–988, 2000.

Hruska, J. Fottova, D. Sach, F. Zmeny V. Chemismu půd a povrchových vod v důsledku dlouhodobé acidifikace Orlických hor. Forestry work No. 10/00 Lesnické hospodaření v imisní oblasti Orlických Hor *Archive of the journal Lesnická práce* 79, 2000.

Hruska, J., Kram, P.: Modelling long-term changes in stream water and soil chemistry in catchments with contrasting vulnerability to acidification Lysina and Pluhuv Bor, Czech Republic, Hydrol. Earth Syst. Sci., 7, 525–539, doi:10.5194/hess-7-525-2003, 2003.

Huntington, T.G.; Ryan, D.F.; Hamburg, S.P: Estimating soil nitrogen and carbon pools in a northern hardwood forest ecosystem. Soil Sci. Soc. Am. J. 52, 1162–1167, 1988.

Jager, E.; Hunzike, J.C.; Eds.; Springer-Verlag, Berlin, pp. 264–273, 1979.

Johnson, J.; Graf Pannatier, E.; Carnicelli, S.; Cecchini, G.; Clarke, N.; Cools, N.; Hansen, K.; Meesenburg, H.; et al.: The response of soil solution chemistry in European forests to decreasing acid deposition, Glob. Chang. Biol. 24, 3603–3619, 2018.

Kram, P.; Hruska, J.; Wenner, B.S.; Driscoll, C.T.; Johnson, C.E.: The biogeochemistry of basic cations in two forest catchments with contrasting lithology in the Czech Republic, Biogeochemistry 37, 173–202. 1997,

Kolar, T.; Cermak, P.; Oulehle, F.; Trnka, M.; Stepanek, P.; Cudlin, P.; Hruska, J.; Büntgen, U.; Rybnicek, M.: Pollution control enhanced spruce growth in the "Black Triangle" near the Czech-Polish border, Sci. Total Environ. 538, 703–711, **2015**.

Kopacek, J.; Hejzlar, J.; Kram, P.; Oulehle, F.; Posch, M. Effect of industrial dust on precipitation chemistry in the Czech Republic Central Europe from 1850 to 2013, Water Res. 103, 30–43, 2015.

Ma, L.; Teng, F-Z.; Jin, L.: Magnesium isotope fractionation during shale weathering in the Shale Hills Critical Zone Observatory, Accumulation of light Mg isotopes in soils by clay mineral transformation. Chem. Geol. 397, 37–50, 2015.

Maloszewski, P.; Zuber, A. Determining the turnover time of groundwater systems with the aid of environmental tracers, J. Hydrol. 573–4, 207–231, doi:10.1016/0022-16948290147-0, 1982.

Manderscheid, B.; Matzner, E.; Meiwes, K.J.; Xu, Y-J.: Long-Term Development of Element Budgets in a Norway spruce (Picea abies, L. Karst) Forest of the German Solling Area, Water Air Soil Pollut. 79, 3–18. 1995.

Manderscheid, B.; Matzner, E.: Spatial and Temporal Variation of Soil Solution Chemistry and Ion Fluxes through the Soil in a Mature Norway-Spruce (Picea abies L. Karst Stand), Biogeochemistry 30, 99–114, 1995.

Matschullat, J.; Andreae, H.; Lessmann, D.; Malessa, V.S.U. Catchment acidification—from the top down, Environ. Pollut. 77, 143–150, 1992.

Mayer, B.; Prietzel, J.; Krouse, H.R.: The influence of sulfur deposition rates on sulfate retention patterns and mechanisms in aerated forest soils, Appl. Geochem. 16, 1003–1019, doi: 10.1016/S0883-2927(01)00010-5, 2001.

McDowell, W.H.; Magill, A.H.; Aitkenhead-Peterson, J.A.; et al.: Effects of chronic nitrogen amendment on dissolved organic matter and inorganic nitrogen in soil solution, Forest Ecol. Manag. 196, 29–41. 2004.

McIntosh, J.C., Schaumberg, C., Perdrial, J., Harpold, A., Vázquez-Ortega, A., Rasmussen, C., Vinson, D., Zapata-Rios, X., Brooks, P.D., Meixner, T., Pelletier, J., Derry, L. and Chorover, J.: Geochemical evolution of the Critical Zone across variable time scales informs concentration-discharge relationships: Jemez River Basin Critical Zone Observatory, Water Resour. Res. 53, 4169–4196, 2017.

Moore, J.; Lichtner, P.C.; White, A.F.; Brantley, S.L.: Using a reactive transport model to elucidate differences between laboratory and field dissolution rates in regolith, Geochim. Cosmochim. Acta 93, 235–261, 2012.

Mörth, C-M.; Torssander, P.; Kjønaas, O.J.; et al.: Mineralization of organic sulfur delays recovery from anthropogenic acidification, Environ. Sci. Technol. 39, 5234–40, 2005.

Navratil, T.; Kurz, D.; Kram, P. et al.: Acidification and recovery of soil at a heavily impacted forest catchment (Lysina, Czech Republic)—SAFE modeling and field results, Ecol. Model. 205, 464–474, doi:10.1016/j. ecolmodel.2007.03.008, 2007.

Novak, M.; Jackova, I.; Prechova, E.: Temporal trends in the isotope signature of air-borne sulfur in Central Europe, Environ. Sci. Technol. 35, 255–260, doi:10.1021/es0000753, 2001.

Novak, M., Kirchner, J.W.; Groscheová, H.; et al.: Sulfur isotope dynamics in two Central European watersheds affected by high atmospheric deposition of SOx, Geochim. Cosmochim. Acta 64, 367–383, doi:10.1016/0022-1694(82)90147-0, 2000.

Novak, M.; Kirchner, J.W.; Fottova, D.; et al.: Isotopic evidence for processes of sulfur retention/release in 13 forested catchments spanning a strong pollution gradient Czech Republic, central Europe, Global Biogeochem. Cycles 19, GB4012, doi:10.1029/2004GB002396, 2005.

Palmer, S.M.; Wellington, B.I.; Johnson, C.E.; Driscoll, C.T.: Landscape influences on aluminum and dissolved organic carbon in streams draining the Hubbard Brook valley, New Hampshire, USA, Hydrol. Proc. 19, 1751–1769, 2005.

Oulehle, F.; Hofmeister, J.; Cudlin, P.; Hruska, J: The effect of reduced atmospheric deposition on soil and soil solution chemistry at a site subjected to long-term acidification, Nacetin, Czech Republic, Sci. Total Environ. 370, 532–544, 2006.

Oulehle, F.; Chuman, T.; Hruska, J.; Kram, P.; McDowell, W.H.; Myska, O.; Navratil, T.; Tesar, M.: Recovery from acidification alters concentrations and fluxes of solutes from Czech catchments. Biogeochemistry 132, 251–272, 2017.

Siegenthaler, U. Stable hydrogen and oxygen isotopes in the water cycle. In Lectures in Isotope Geology; Jager, E.; Hunzike, J.C.; Eds.; Springer-Verlag, Berlin, pp. 264–273, 1979.

Schoumans, O.F.: Determination of the degree of phosphate saturation in non-calcareous soils. In Methods of Phosphorus Analysis in Soils, Sediments and Waters; Pierzynski, G.M., Eds.; North Carolina State University, Raleigh, NC, USA; pp. 31–34, 2000.

van Miegroet, H.; Cole, D.W. The impact of nitrification on soil acidification and cation leaching in a red alder Alnus rubra ecosystem. J. Environ. Qual. 13, 586–590 1984.

Vega, M.; Pardo, R.; Barrado, E.; Deban, L.: Assessment of seasonal and polluting effects on the quality of river water by exploratory data analysis. Water Res. 32, 3581–3592, 1998.

Wesselink, L.G.; Meiwes, K.J.; Matzner, E.; Stein, A.: Long-term changes in water and soil chemistry in spruce and beech Forests, Soiling, Germany, Environ, Sci. Technol. 29, 51–58, 1995.

Winchester, J.A.; Pharaoh, T.C.; Verniers, J.: Palaeozoic amalgamation of Central Europe. Geol. Soc. London, Spec. Pubs. 201, 237–277, 2002.
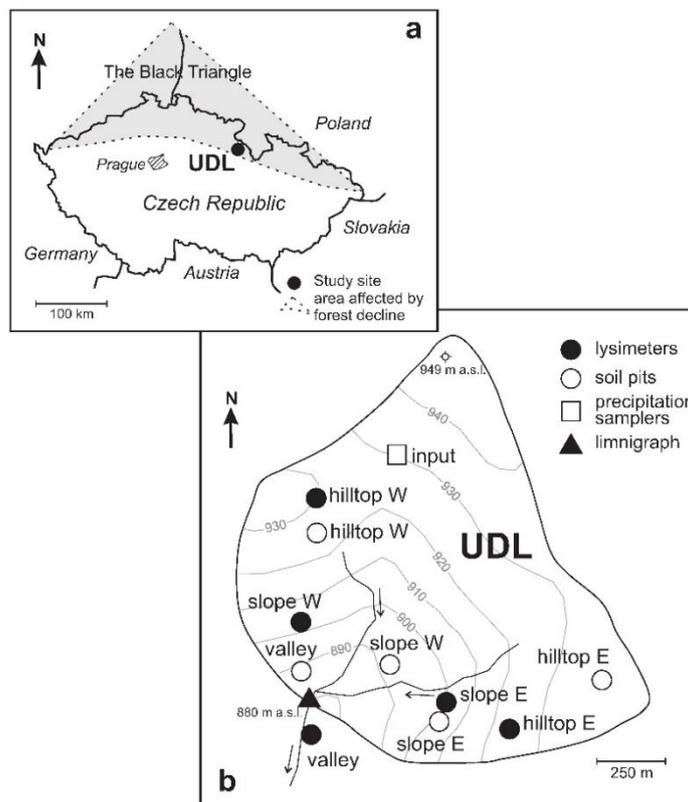
Figure 1: Study site location: (a) The shaded area shows the so-called "Black Triangle", (b) Sampling setup. In the studied UDL site, spruce stands die-back at elevations > 700 m a.s.l. due to acid rain between approximately 1975 and 1996.
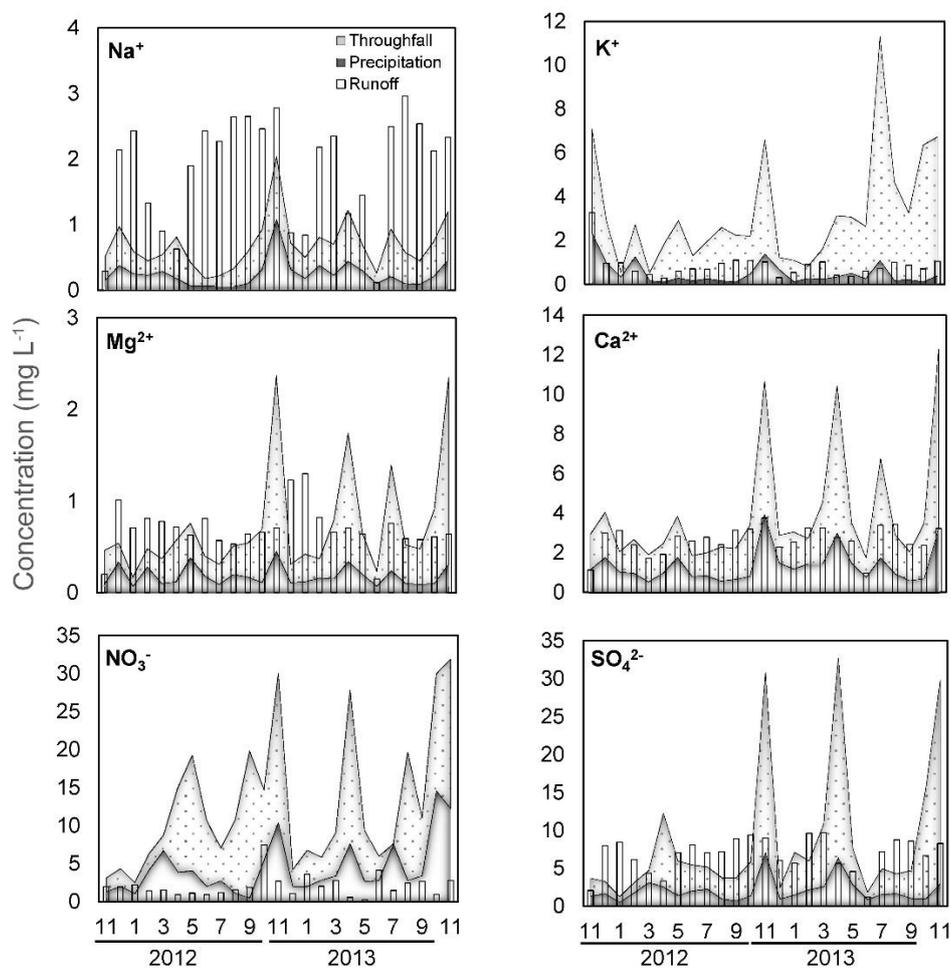
Figure 2: Hydrochemical data relevant for the monitoring period (2012-2013). X-axis shows months and hydrological year; concentrations after Oulehle et al. (2017).
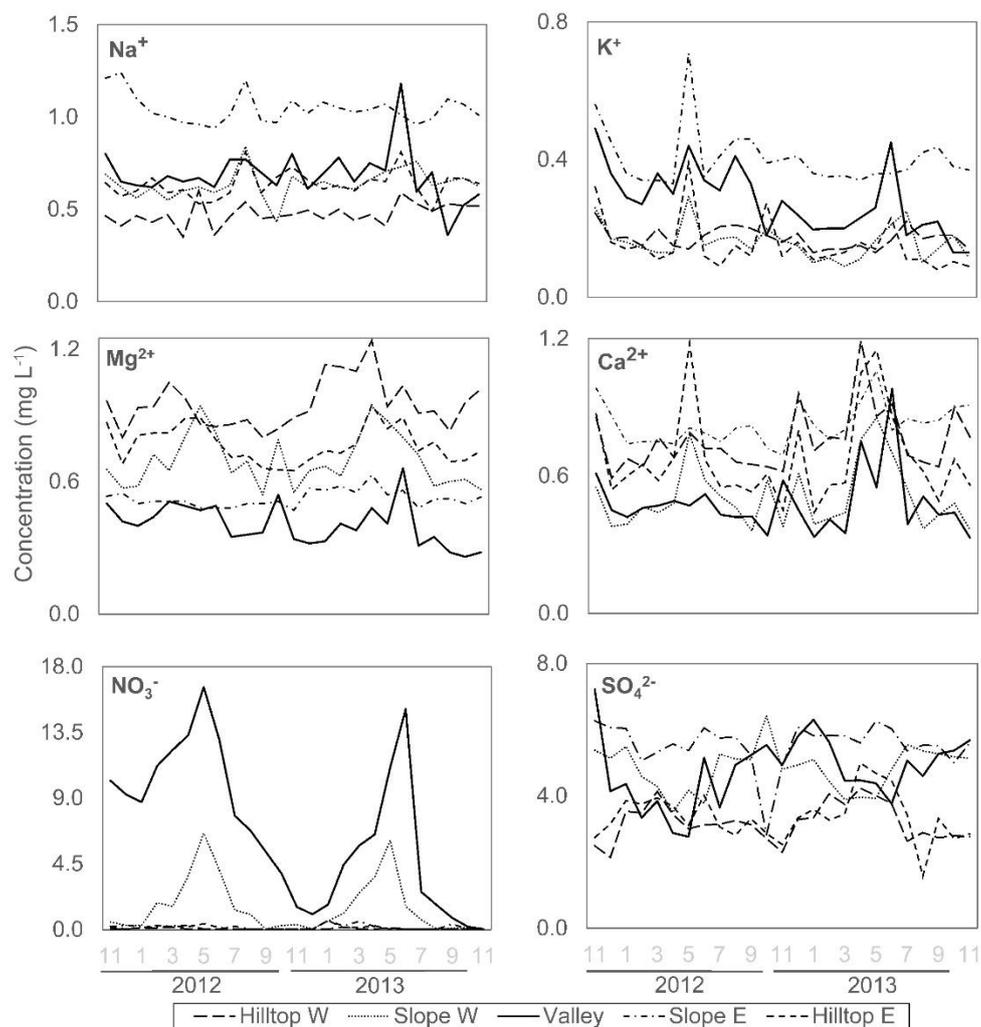
Figure 3: Spatially resolved, time-series soil water concentration values of base cations, sulfate and nitrate at 50-cm depth. X-axis shows months and hydrological year.
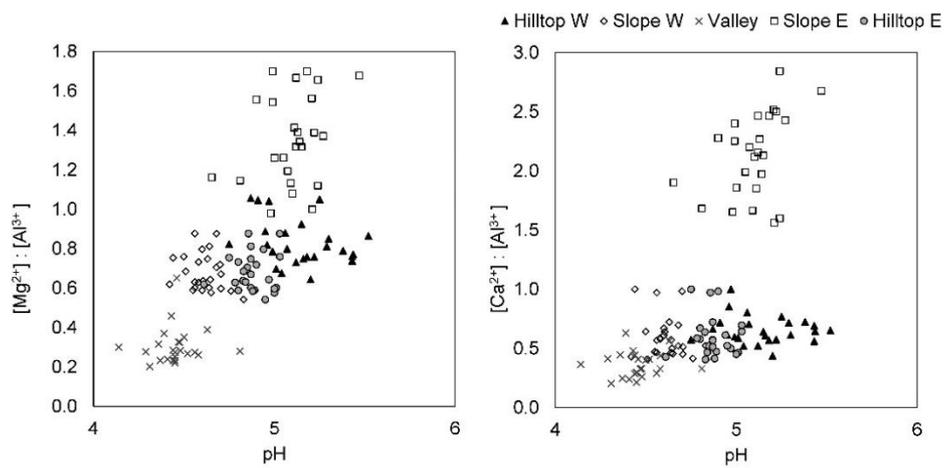
Figure 4: Comparison of Ca/Al and Mg/Al *vs.* pH.
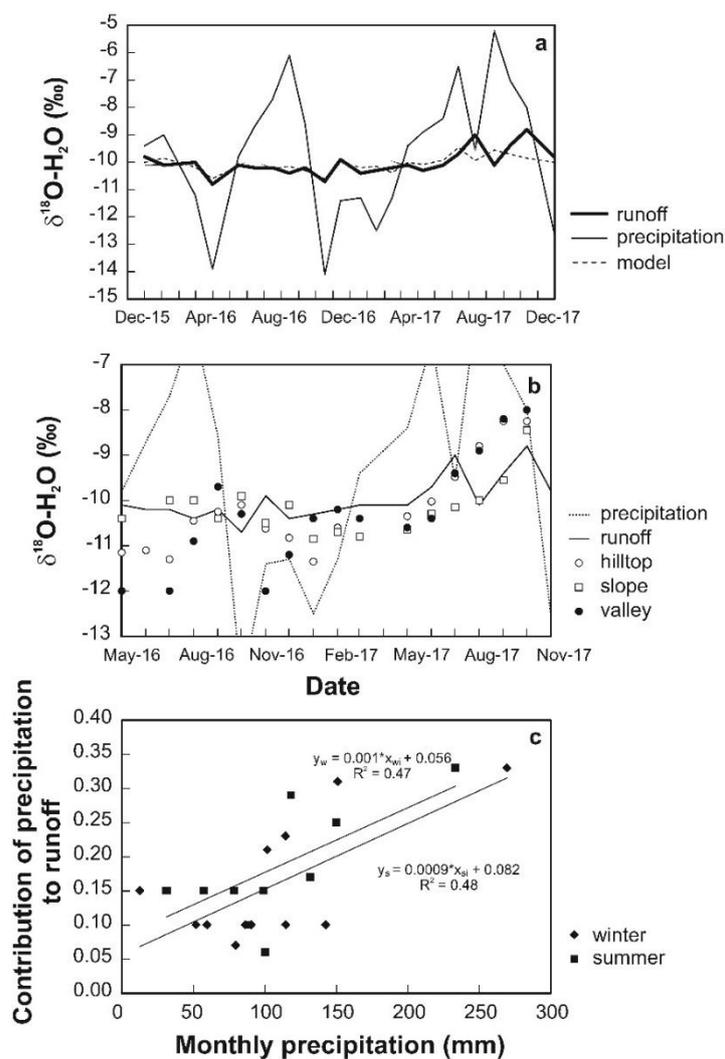
Figure 2A: Time series of $\delta^{18}O$: (a) input-output model. (b) Areal distribution across the UDL catchment. (c) Estimated contribution of precipitation in runoff.

Table 1. Average hydrochemical data 2012-2013 (after Oulehle et al., 2017)

	pH	SO$_4^{2-}$	NO$_3^-$	NH$_4^+$	DOC	Na$^+$	K$^+$	Mg^{2+}	Ca^{2+}	Al^{3+}	TP
					μg L^{-1}						
Rainfall	5.7	2000	4400	700	2200	5700	500	200	1350	NM	< 20
Throughfall	5.5	6590	8490	1930	7310	445	2760	551	2600	NM	< 20
Runoff[#]	5.9	6840	2070	40	7230	1850	842	699	2660	305	21.4

[#]Average runoff flux during the monitoring period was 9.4 L s^{-1}, with maximums recorded in April (76.9 ± 4.0 L·s^{-1}) and minimums in August (0.5 ± 0.1 L s^{-1}). NM: not measured

Table 2. Spatially resolved physical and geochemical data for solid substrate (40-80 cm depth) and annual average soil water chemistries at the 50-cm depth

Measurement	Hilltop W		Slope W		Valley		Slope E		Hilltop E	
Soil										
CEC (meq kg^{-1})	19.4		22.6		27.2		33.4		58.4	
BS (%)	7.5		6.4		7.7		9.2		12.5	
>10 cm (t ha^{-1})[‡]	0		75		0		141		2038	
< 2-mm (t ha^{-1})[‡]	4707		2842		2199		3726		1102	
pH$_{H2O}$	4.2		4.6		4.7		4.7		4.4	
Na (mg kg^{-1})	3		6		17		6		34	
K (mg kg^{-1})	30		19		4		29		7	
Mg (mg kg^{-1})	2		8		4		9		27	
Ca (mg kg^{-1})	7		27		20		26		78	
C$_{org}$ (%)	0.40		0.81		0.99		0.45		1.81	
TN (%)	0.020		0.037		0.045		0.032		0.101	
Al$_{Ox}$ (mg kg^{-1})	3880		5490		4390		2550		2370	
Fe$_{Ox}$ (mg kg^{-1})	1040		2500		3950		2810		4150	
P$_{Ox}$ (mg kg^{-1})	352		421		334		450		536	
DPS$_{Ox}$[#]	0.14		0.10		0.08		0.17		0.16	
Measurement	2012	2013	2012	2013	2012	2013	2012	2013	2012	2013
Soil solution*										
pH	5.4	5.5	4.6	4.4	4.1	4.5	5.0	4.8	4.9	4.9
SO$_4^{2-}$	3132	3270	4850	4770	4420	5000	5440	5640	3360	3400
NO$_3^-$	63	58	1800	1300	9870	4040	155	181	149	117
NH$_4^+$	< 20	< 20	< 20	< 20	< 20	30	< 20	< 20	< 20	70
DOC	13500	NA	8440	NA	4510	NA	4230	NA	15100	NA
Al^{3+}	1130	1170	945	859	1590	1280	396	394	1130	1150
Na$^+$	455	493	611	662	683	687	1050	1040	618	649
K$^+$	184	161	177	145	340	225	430	378	179	128
Mg^{2+}	897	1000	700	699	445	378	505	539	775	764
Ca^{2+}	699	806	498	531	459	514	794	851	668	697
Conductivity	18.8	19.8	27.0	26.5	43.0	33.2	23.6	22.5	20.6	20.6

[‡] Soil particulate size. [#] Degree of P Saturation (DPS = P$_{ox}\cdot(0.5\cdot(Fe_{ox} + Al_{ox})^{-1})$). *Concentrations in μg L^{-1}; conductivity in μS cm^{-1}. NA: not measured.